

Interactive comment on “Reconstructing volcanic plume evolution integrating satellite and ground-based data: Application to the 23rd November 2013 Etna eruption” by Matthieu Poret et al.

Matthieu Poret et al.

matthieu.poret@gmail.com

Received and published: 28 February 2018

Comments from Larry Mastin (Referee 1)

Main comments

This paper combines deposit mass load data, radar data, and satellite data to reconstruct the grain-size distribution of erupted material from the 23rd November 2013 paroxysmal eruption of Etna volcano, Italy. Reconstruction of grain-size distributions during eruptions is important for modelling and forecasting tephra hazards. But it is

C1

laborious, requiring systematic sampling of a tephra deposit and integrating grain-size data. Grain-size data collected from a tephra deposit is also incomplete, because a significant (and usually unknown) fraction of the erupted mass drifts downwind, to distances far beyond the mapped deposit. Few studies have attempted to estimate the fraction of the deposit escapes the mapped area. Yet it is a key input in ash-cloud models used for aviation safety. This is one of very few studies that integrates deposit, radar, and ash-cloud data to derive a complete grain-size distribution (TGSD). For this reason, I support its publication. However, before recommending publication I think it requires significant revision. In particular:

1. Explanations are too long, complicated, and frequently unclear. Many examples are flagged in the accompanying pdf. The revised manuscript should be reviewed again to ensure that it can be understood.

Answer: The manuscript was modified keeping in mind the necessity to improve the clarity of the explanations. We hope the revised manuscript is easier to understand.

2. Much of the methodology is not clearly explained. Or at least I had trouble following it. Key issues are:

a. One or more tables should be added summarizing inputs, including model domain, nodal spacing, etc.

Answer: We added a table (now Table 2) to report the input parameters with the corresponding ranges. Also, we added an Appendix to summarize the parameterization used for the simulations under the 2 different meteorological databases.

b. There should more explanation (perhaps in a table) of which parameters are changed in each simulation, and how they are changed. In Table 2 for example, I had assumed that the only parameters changed from one row to the next were the relative percentages of the deposit-based TGSD and the radar-based TGSD. But it appears that the total erupted mass is also changing. Why? Is the mass being adjusted

C2

to optimize the fit? Does each TGSD have an erupted mass associated with it?

Answer: We modified the text in p.7 - lines 12-16 to precise which parameters were modified in each simulation. We also added a table (now Table 2) to report the input parameters with their ranges. The Integrated TGSD was inverted by comparing each tested weighting average combination. For that reason, we reported in Table 3 the best simulations (i.e. optimal α and β) for all the combinations selected on the basis of the goodness-of-fit procedure (i.e. $K \approx 1$), explaining the resulting different TEM estimations. The latter point was described in p.9 - lines 36-39.

c. Section 3.1 should more fully explain how the radar retrievals are combined to give a TGSD. The radar returns a reflectivity (which can be turned into GSD) for each volume, delineated by horizontal angle, vertical angle, range, and time. How are these combined to give a TGSD for the entire eruption?

Answer: Thank you for having pointed out the lack of information. Actually, we considered a spatial and temporal average of the X-Radar-based GSD (referred as PSD: particle size distribution in the main text) to obtain the TGSD for the whole event. The average takes in input each PSD estimated from each single radar resolution volume delineated by horizontal angle, vertical angle, and range distance at each available time step. We modified the text in p.5 - lines 1-13.

d. Section 3.2 should clarify how FPlume output feeds into FALL3D. A list of inputs for FPlume, and another list of its outputs that go into FALL3D, would be helpful.

Answer: Thank you for having pointed out the issue. We clarified the section (p.5 - lines 33-41) to better explain how FPlume and FALL3D work together. Additionally, we added a table (now Table 2) to show the key input parameters.

e. Please explain the Poret et al. (2017) method of inverting for alpha and beta (p. 6, line 12). Do you hold plume height and eruption rate constant (using independent information) and then optimize alpha and beta? What range of alpha and beta do you

C3

start with before you optimize? Your resulting values, 0.06-0.15 for alpha and 0.2 to 1.0 for beta, are so broad that I'm not sure the inversion is worth including.

Answer: Section 3.3 was modified to better describe the inversion procedure, especially for α and β . As mentioned in p.7 - lines 12-16, we hold the column height and inverted α and β following the goodness-of-fit procedure (i.e. RMSEs, K , k ...). The resulting ranges are broad but are regardless to the weighting average combination. The α and β values obtained after inversion for each weighting average combination were added in Table 3 and reported in P.9 - lines 5-7.

f. What factor(s) determine the vertical distribution of mass with height in the FALL3D model? Is this an output from FPlume, or do you use some parameterization, like a Suzuki curve?

Answer: We did not use Suzuki's parameterization. In fact, we used the FPlume model to determine the vertical mass distribution. The model uses the air mixing entrainment coefficients (i.e. α and β) to distribute vertically the mass (Folch et al., 2016). We modified p.5 - lines 33-41 to clarify how FPlume feeds FALL3D.

3. It would be of great value to discuss some results in the context of other studies. Most significant (in my opinion) is your finding that the mass fraction of fine ash (PM20) is 3.6-9.0 wt% of the erupted mass. This fraction is a critical input into ash-cloud models used for aviation safety because it is the mass that goes into the downwind cloud. Few studies have constrained it. NOAA's Hysplit model assumes for example that 5% of the erupted mass makes it into the downwind cloud and uses this 5% as model input. At Spurr in 1992, Wen and Rose [1994] estimated about 2% of the erupted mass went into the distal cloud. At Eyja, the estimates range from 0.9% to 11% [Bonadonna et al., 2011; Dacre et al., 2011; Devenish et al., 2012]. Basaltic eruptions like Etna tend to be very poor in fine ash, hence I would expect a lower fraction. But your 3.6-9 wt% are in the middle of the previous numbers. Does this mean that we don't need to adjust downward when modelling a basaltic eruption? Additional comments are below, and in

C4

the attached pdf. Some duplicate points made above. Overall, I think the paper merits publication. But it should be revised to shorten, clarify, improve readability, and explain methods. I look forward to seeing the final version.

Answer: Probably there was a misunderstanding on this point. These eruptions are not comparable among them as the fraction of fine ash is very different from one case to the other. It can range from 50% to a few %. The fact that Hysplit or other model assume fraction of about 5% is not related with what we estimate for the Etna eruption. In the former case, 5% would represent the fine ash fraction that escape to aggregation processes and travel far away. In the case of basaltic eruptions fine ash content is lower and hence aggregation less efficient, implying that almost all the fine ash fraction can be transported distally. In the revised version we briefly discussed this point (p.10 - lines 40-42 - p.11 - lines 1-12).

Specific comments

Page 3, line 16, and Figure 2: Is there any evidence that the existence of a whitish plume on top and grayish below was persistent during the eruption? Or is this photo just recording a transient phenomenon? Also, the upper cloud looks light gray to me, not exactly white, like the one in the lower right of Fig. 2.

Answer: The plume was observed by cameras from the INGV-OE through visible images that showed the 2 plumes, the greyish above the brownish one. We understood the confusion about the colour name. We replaced "whitish" by "greyish" (p.3 - line 8).

p. 3, line 26. What method(s) does the CAMSIZER use for grain-size analysis? Laser? Settling rates? Some combination?

Answer: The CAMSIZER measure optically the grain-size, which was mentioned in p.3 - line 17.

Section 2.1 (page 3): The number of samples collected (7) is pretty small. Thus, there is a strong chance of bias in your results. Can describe where the samples were taken

C5

relative to the dispersal axis, and how (or whether) you know the overall distribution of the deposit?

Answer: Although a set of 7 samples is a relatively small number, we used the field data as a starting point from which we added radar and satellite data. Moreover, such a small number of samples is common for Etna eruptions. The study does not assume the samples are located within the main axis of the plume, but compares the simulation outputs with the field data, best-fitting the sampled tephra loadings. We do not know the overall distribution, but we based this study on reproducing the field measurements together with the airborne ash observations. In addition, the field-derived TEM is compared to the FALL3D results. We believe that the synergic use of these points increases the relevance of our findings.

p. 3, lines 31-32: The MER estimate of 4.5×10^6 kg/s for the climax phase comes from the mapped deposit and observed duration. Where does the estimate of 1×10^6 kg/s come from?

Answer: In p.3 - line 23, the $MER = 4.5 \pm 3.6 \times 10^5$ kg/s comes from the estimation made in Andronico et al. (2015) and refers to the entire paroxysm (~50 min). The value of 10^6 kg/s concerns the maxima reached during the climax phase (i.e. from 09:55 to 10:14; ~19 min) and comes from Donnadieu et al. (2017).

p. 4, line 21. How do you derive a mass eruption rate from radar? From plume height using FPlume?

Answer: In p.4 - line 12, Corradini et al. (2016) reported the total erupted mass not the mass eruption rate. In this study, we have not used the radar data to derive the MER.

p. 4, lines 23-24. I'm getting a little confused about the release of the ice and ash clouds. On p. 3, you seemed to imply that ash and moisture (forming the ice cloud) were released at the same time but at different elevations. Here you seem to be saying that they came out at different times (but maybe overlapped in time).

C6

Answer: In p.3 - lines 39-41 - p.4 - lines 1-8, we described the satellite retrievals in terms of mass. We mentioned that ash dominates first in mass, and then ice (produced from the release of water vapour). In Fig. 4, the time discrepancy between ash and ice mass peaks is due to the release of the water vapour coupled with the required time to produce ice from water vapour. To avoid confusion, we clarified the point (p.4 - lines 5-6).

p. 4, lines 10-28. This paragraph needs to be reorganized and reworded to improve its coherence.

Answer: The confusing paragraph was reworded and reorganized in 2 paragraphs to gain in clarity helping the reader to follow the flow (p.3 - lines 38-41 - p.4 - lines 1-15).

Equation 1: Does this equation assume that the plane of the block's trajectory is the same as that of the radar beam? If not, I don't see how that the angle between the two is considered. Also, why is ejection velocity important in this study? It is not really related to column height, or MER. Is it just a qualitative indicator of eruption intensity?

Answer: Equation 1 is used to calculate the ejection velocity from the near-source detection retrievals of the L-band radar. The equation assumes that block's trajectory is vertical, which is considered by means of the elevation angle of the radar beam ($\theta=14.9^\circ$). Regarding the use of the ejection velocity data (VOLDORAD 2B), we worked on discretizing the eruption into several phases to best fit the column height observations. From a numerical point of view, we described a phase by a time interval, a column height value, and an average ejection velocity.

P. 5, lines 8-15. This explanation should be reworded to be clearer and more concise. I don't have specific suggestions. But I think you are saying that the field TGSD will be biased toward coarse ash, and that the radar will help constrain the mass of fine ash.

Answer: The explanation was corrected trying to be clearer and concise as suggested (p.4 - lines 35-40 - p.5 - line 1). The main point was to mention that the field-derived

C7

TGSD cannot represent the full size-spectrum TGSD and needs to be improved prior use within the FPlume and FALL3D models.

p. 5, lines 19-29. You talk about estimating TGSD from the radar. So, you estimate two independent TGSD's? One from the deposit and another from radar? Perhaps this should be mentioned. It is not clear to me how you derive a TGSD.

Answer: The paragraph was unclear and was modified to mention clearly and concisely the estimation of the TGSD from the field measurements (p.4 - lines 35-40) and the X-Radar retrievals (p.5 - lines 1-13).

Section 3.1 (p. 5). There is some critical information I don't see in the explanation of TGSD derived from radar. I assume that the radar provides a TGSD for each volume, delineated by range, and horizontal and vertical angles, and time of the scan. Somehow these volumes are integrated to get a radar-based TGSD for the entire airborne mass. How is this done?

Answer: As mentioned above, we considered a spatial and temporal average of the X-Radar-based GSD (referred as PSD: particle size distribution in the main text) to obtain the TGSD for the whole event. The average takes in input each PSD estimated from each single radar resolution volume delineated by horizontal angle, vertical angle, and range distance at each available time step. We modified the text in p.5 - lines 1-13.

p. 5, lines 27-28: "To [integrate the radar and field TGSDs], we investigated the weights at regular intervals until we best-fit the field measurements maintaining the shape of the radar TGSD on the proper grain-size interval". After reading this sentence a couple of times, I'm still not sure exactly how you arrived at a best fit. You adjusted the relative amounts of radar ash and field ash until the heights of the histogram bars in the overlapping interval agreed?

Answer: The sentence was confusing. We modified the sentence with the previous ones to better explain the procedure used for estimating the Integrated TGSD (p.5

C8

- lines 14-20). Such a TGSD is obtained by testing the relative weighting averages from 100% Field TGSD to 100% Radar TGSD. The best-fit is reached when the field measurements are best reproduced following a goodness-of-fit procedure (Sect. 3.3).

p. 5, line 36. "X(ϕ_5) is the fraction obtained for $\phi=5$ ". How do you obtain this fraction? By estimating the total mass of the cloud and dividing it by the total mass of the deposit+cloud? Also, there could be a little more explanation about how PM20 is estimated from the integrated TGSD. If PM20 is at the tail of the size distribution derived from radar, it seems that the mass of PM20 would be highly dependent on the size distribution assumed (i.e. γ) from the radar retrievals. TGSD's tend to be polymodal, a fact that is not considered here.

Answer: The paragraph (p.5 - lines 21-31) was reworked to gain in clarity about the empirical modification of the Integrated TGSD. We based the modification on the power-law decay, starting from $\Phi = 6$ (i.e. PM20). In other words, the fractions for $-5 \leq \Phi \leq 5$ are determined by applying the relative weighting factors to the Field and Radar TGSDs, without modifying the individual TGSDs. The paragraph related to the weighting average inversion is mentioned in p.5 - lines 14-20. As described in Costa et al. (2016a), the polymodality on TGSD tends to be a common feature for most eruptions. The issue associated with the distribution used for radar retrieval (Gamma distribution) has been described (p.5 - lines 7-13) and a better characterization of such distribution is the subject of ongoing research. In particular, as we explained in p.5 - lines 1-7, the Gamma distribution is assumed for the variables D and ND, where D(mm) is the particle diameter and N ($\text{mm}^{-1} \cdot \text{m}^{-3}$) is the number of particles per unit of volume and particle size interval. Then, this distribution is converted in Φ , wt %. In addition, since a single Gamma distribution is not able to adequately describe large size spectra, a Gamma distribution, with different parameters, is assumed in each particle size range of fine ash, coarse ash, small lapilli, and large lapilli, so the final total distribution is a combination of several Gamma distributions. However, such an empirical derived distribution can be probably approximated using distributions different than the Gamma distribu-

C9

tion, such as a lognormal or a Weibull distribution. The latter point will be investigated in future studies.

p. 6, line 12: " α and β are obtained empirically through the solution of an inverse problem (Poret et al., 2017)". A little more detail would be helpful. You took cases where both the plume height and eruption rate were known, and then adjusted α and β until the modeled height matched the observed one?

Answer: Throughout the simulations, we hold the column height (hence MER). The sentence was modified (p.6 - lines 2-6) to better explain how the air entrainment coefficients were used. More details on the calibration were given in the following section (e.g. p.7 - lines 12-16) about the inversion modelling strategy. α and β are inverted on the basis of the theoretical erupted mass estimated from the field samples (p.7 - lines 23-26). We used α and β ranges to make the index K converging towards 1 giving the optimal erupted mass.

p. 6, lines 24-42. The English in this paragraph really needs some work. And why are you spending so much time comparing winds over the volcano with those in Tirana?

Answer: The paragraph was reworked to edit the read (p.6 - lines 20-39). We used few lines to compare the wind conditions over the two different locations to 1) justify the benefit from such meteorological conditions during the eruption (i.e. wind speed and direction), and 2) the alternative use of the 2 meteorological databases.

Section 3.3 (p. 6, lines 10+). I think it would be valuable to show a table listing variables that were varied in your optimizations.

Answer: Thank you for pointed out the lack of visibility. We added a table to list the input parameters (now Table 2). We also edited Section 3.3 to read (p.7 - line 5).

p. 7, line 15. To quantify the goodness of fit, what observations were you comparing with model results? Cloud load? Deposit mass load? Was each observation, e.g. deposit mass load at each sample location, equally weighted with every other obser-

C10

vation? Also, there is not enough explanation of K and k to know what they signify. It would be worthwhile to show the equations used to calculate K and k .

Answer: The comparison description was confusing. We mentioned the comparison of the tephra loadings at the sampled sites between the numerical outputs and the field measurements (p.7 - lines 10-11). Also, we clarified the goodness-of-fit procedure in p.7 - lines 17-27, and added the equations defining the indexes K and k .

p. 7, line 25. It's not exactly clear to me what simulations you are doing that attempt to reproduce "sampled tephra loadings". Are you doing plume simulations, feeding the airborne tephra into FALL3D to simulate the deposit, then comparing the simulated deposit mass load with measured values? What were the setup parameters for the FALL3D runs? What was the model domain, model resolution etc.?

Answer: We computed the tephra loading at the sampled sites, which are compared with the field measurements (p.7 - lines 10-11). We added a table listing the input parameters (now Table 2) and an Appendix indicating the complementary parameterization used within FALL3D.

p. 9, lines 8-9. What FPlume results were you comparing with observations during your simulations that constrained values of α and β ? The constrained ranges, $\alpha=0.06-0.15$, $\beta=0.21-1.00$, are so wide that I think the constraints aren't really meaningful.

Answer: To constrain the parameters α and β , we compared the tephra loading at the sampled sites. During the inversion of the Integrated TGSD, we tested the relative weighting averages for the Field and Radar TGSDs between 100% Field TGSD and 100% Radar TGSD. For such interval, we obtained α and β ranging from 0.06 - 0.15 and 0.21 - 1.00, respectively. To retrieve the best weighting average combination for the Integrated TGSD, we compared the optimal simulations in terms of theoretical TEM for all the combinations (now Table 3). For this reason, we obtained various α and β values also reported in Table 3. As a consequence of running simulations for each weighting

C11

average combination, and different α and β values, the resulting TEM also varied (Table 3). Although the different Integrated TGSDs tested contain variable amount of coarse and fine ash, the results yield range for α and β consistent with the literature (p.9 - lines 5-7).

p. 9, lines 25-30. There are several reasons why the model result could be inaccurate in the proximal region. One of them has to do with details of plume dynamics, and fallout of large clasts from the side of the rising column. How is FPlume integrated into FALL3D? Does it consider fallout from the side of the column? How does it transfer mass from the column to FALL3D? How is fine ash distributed with height? Is this determined within FPlume, and then transferred to FALL3D for lateral transport?

Answer: Among the different input parameters FPlume uses TGSD to solve mass conservation equation for each class and distribute it along the column. Then the mass related to the different particle classes at each different level is transported laterally using FALL3D. This was added in the revised version (p.5 - 33-41).

p. 10, line 8. You note here that the assumptions involved in the radar analysis add uncertainty. It would help to be specific about which assumptions are important, and how they would affect uncertainty.

Answer: X-Radar retrievals suffer from uncertainty essentially due to three main factors: radar forward model parameterization, geometry of view and instrument calibration. Although all of them are important, a complete sensitivity study on the error sources associated with X-Radar retrievals is not yet available for the community and is beyond the scope of this work. However, instrument calibration has been checked and corrections applied before processing data for the final estimation. The limitations of the geometry of view must be accepted for obvious reasons. An important role is played by the radar forward model parameterizations, which are used to reproduce synthetic signature of radar observations, and then considered to set up the retrieval algorithm. In this respect, among others assumptions (particle shape, density, and

C12

orientation) we assumed a Gamma shaped PSD and Rayleigh particle's scattering regime to retrieve PSD parameters. Our feeling is that radar forward model assumptions mainly drive the final radar retrieval. We corrected the sentence in p.10 - lines 4-7.

Table 2: What are RMSE_1, RMSE_2, and RMSE_3? RMSE values for each of the three eruption schemes illustrated in Fig. 7? Also, I'm a bit confused about why the total erupted mass (TEM) is changing in each row of the table. Are you adjusting it until the RMSE is minimized? Are you adjusting any other parameters? Are you somehow calculating the total mass in the air from radar measurements and using that as the model input? This reinforces my view that there is a lot that needs to be explained regarding the radar data.

Answer: The different RMSEs are introduced in p.7 - lines 18-19. They refer to different error distributions as described in Folch et al. (2010). The table (now Table 3) was not well introduced, which is corrected in p.8 - line 20 (Section 4.1). We also mentioned that each combination in the table refers to the input parameter values (e.g. α and β) used to obtain the best theoretical TEM ($K \approx 1$), explaining the report in Table 3 of TEM for each weighting combination. Then, in p.9 - lines 34-39, we discussed the resulting output TEMs with the values from the literature (Andronico et al., 2015; Corradini et al., 2016).

Figure 5: Isn't the radar TGSD supposed to have a gamma distribution? It doesn't look like one. (or does the gamma distribution only apply to each volume in the radar?).

Answer: As mentioned above, the Gamma distribution has a Gamma shape in the D, ND domain, where D (mm) is the particle's diameter and N (mm⁻¹.m⁻³) is the number particles per unit of volume and particle's size interval. This is why you probably do not recognize a Gamma distribution in Fig. 5, which is displayed in Φ (wt%). In addition, since a single Gamma distribution is not able to adequately describe a large size-spectra, a Gamma distribution (with other parameters) is assumed for each particle

C13

size range of fine ash, coarse ash, and lapilli. It follows that the final total distribution is a combination of several Gamma distributions.

Animation A1: How were the SEVIRI data processed to give ash mass load? Who did the processing? Why does the animation look like a model output? Should it show pixels of ash? Why is there a brown airplane off the coast of Albania?

Answer: Thank you for pointed out the confusion. We tried to display the SEVIRI retrieval time-series over the DEM to be consistent with the other animations. We corrected the animation providing the SEVIRI retrievals.

References

Bonadonna, C., R. Genco, M. Gouhier, M. Pistolesi, R. Cioni, F. Alfano, A. Hoskulds-son, and M. Ripepe (2011), Tephra sedimentation during the 2010 Eyjafjallajökull eruption (Iceland) from deposit, radar, and satellite observations, *J Geophys Res*, 116,doi 10.1029/2011jb008462. Dacre, H. F., A. L. M. Grant, R. J. Hogan, S. E. Belcher, D. J. Thomson, B. Devenish, F. Marengo, J. Haywood, A. Ansmann, and I. Mattis (2011), The structure and magnitude of the ash plume during the initial phase of the Eyjafjal-ajökull eruption, evaluated us- ing lidar observations and NAME simulations, *Journal of Geophysical Research*, 116, D00U03,doi 10.1029/2011JD015608. Devenish, B., P. N. Francis, B. T. Johnson, R. S. J. Sparks, and D. J. Thom- son (2012), Sensitivity analysis of dispersion modeling of volcanic ash from Ey- jafjallajökull in May 2010, *Journal of Geophysical Research*, 117(D00U21),doi doi:10.1029/2011JD016782. Wen, S., and W. I. Rose (1994), Retrieval of sizes and total masses of particles in volcanic clouds using AVHRR bands 4 and 5, *Journal of Geophysical Research*, 99(D3), 5421-5431.

Please also note the supplement to this comment:

<https://www.atmos-chem-phys-discuss.net/acp-2017-1146/acp-2017-1146-AC1-supplement.zip>

C14

C15

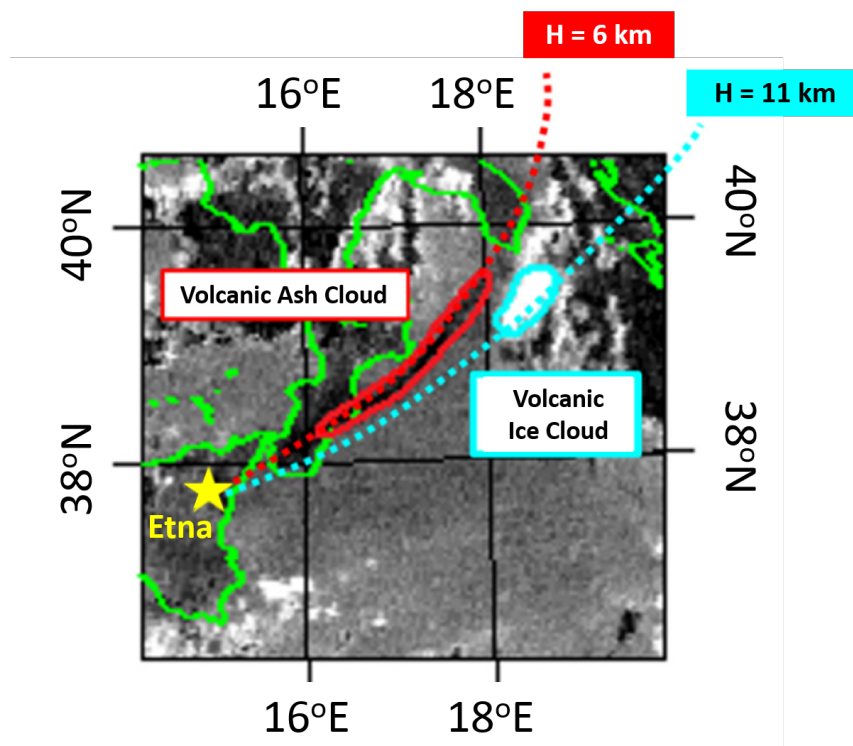


Fig. 1. Figure 3: Satellite image (SEVIRI) showing the trajectories of the two volcanic clouds (modified from Figure 17 in Corradini et al., 2016). The ash cloud dispersed towards the Puglia region (southern

C16